

TOWARD A LAMINAR-FLOW-CONTROL TRANSPORT FOR THE 1990'S*

R. F. Sturgeon
Lockheed-Georgia Company

SUMMARY

Analyses were conducted to define a practical design for an advanced technology Laminar-Flow-Control (LFC) transport for initial passenger operation in the early 1990's. Included in these analyses was the definition of mission requirements, appropriate design criteria, and level of technology for the study aircraft. The characteristics of the selected configuration were established, aircraft and LFC subsystems compatible with the mission requirements were defined, and the aircraft was evaluated in terms of fuel efficiency. A wing design integrating the LFC ducting and metering system into advanced composite wing structure was developed, manufacturing procedures for the surface panel design were established, and environmental and structural testing of surface panel components were conducted. Test results revealed a requirement for relatively minor changes in the manufacturing procedures employed, but have shown the general compatibility of both the selected design and the use of composite materials with the requirements of LFC wing surface panels.

INTRODUCTION

Of all advanced technology concepts currently under consideration for application during the next two decades, Laminar-Flow-Control (LFC) offers the greatest potential for improving the efficiency of long-range transport aircraft. In operation, this efficiency improvement may be translated into reduced fuel consumption or improved payload/range performance.

Both the theoretical methods and engineering and design techniques requisite to the application of LFC have been reasonably well-known since the mid-1940's. The validity of this background and the potential of LFC were partially evaluated in the 1960-1966

* This paper is based on studies conducted under Contract NAS1-14631, "Evaluation of Laminar-Flow-Control System Concepts for Subsonic Commercial Transport Aircraft," sponsored by the NASA Langley Research Center, Hampton, Virginia.

period by Northrop as a part of the X-21A LFC Demonstration Program (ref. 1-4). Recent studies, described in reference 5, have evaluated the potential economic advantages of LFC in the projected airline environment. However, a conclusion common to all previous evaluations is that significant advances are required in both the development of basic design criteria and in the operational verification of LFC prior to the incorporation of this technology on a production transport. The current LFC development program, sponsored by the NASA as one element of the Aircraft Energy Efficiency Project, is directed toward the satisfaction of these requirements. The contracted study on which this paper is based is one of several current efforts included in the first phase of the LFC development program.

As a part of the subject contract, an advanced technology LFC transport configuration was developed for a design mission range of 12,038 km (6500 n mi) and a payload of 400 passengers. The resultant configuration, which will be used in subsequent study phases for the evaluation of alternative LFC system concepts, has optimum configuration geometry for the design mission. While all elements of the LFC systems installation have not been optimized at this point in the study, the configuration is representative of a practical advanced technology commercial transport compatible with initial operation in the early 1990's.

The analyses conducted in the process of selecting the aircraft configuration and the pertinent characteristics of the selected aircraft are described. Included as a part of these analyses is a definition of the mission requirements, pertinent design criteria, and the level of technology assumed for the aircraft. The selected aircraft geometry, engine, and operational parameters are outlined, and the characteristics of the study configuration are defined.

In addition to the general discussions devoted to overall aircraft characteristics, the investigations completed in the development of LFC wing structural concepts are described. A wing design integrating the LFC ducting and metering system into advanced composite wing structure, manufacturing procedures for the design concept, and environmental and structural testing of surface panel components are described. A variety of test results are summarized.

SYMBOLS AND ABBREVIATIONS

Values are given in both SI and U. S. Customary Units. The measurements and calculations were made in U. S. Customary Units.

b	slot duct width, mm (in)
C_p	pressure coefficient
d	metering hole diameter, mm (in)

g	acceleration of gravity
h	slot duct depth, mm (in)
H_s	pressure on wing surface at slot entry, N/m ² (lb/in ²)
M	Mach number
M_D	design dive Mach number
P	absolute pressure, N/m ² (lb/in ²)
R_N	chord Reynolds number
s	metering hole spacing, mm (in)
V_D	design dive speed, knots
W/S	wing loading, kg/m ² (lb/ft ²)
x/c	chord location
y	metering hole offset, mm (in)
η	cruise power ratio
Λ	wing sweep, rad (deg)
Λ_{LE}	wing sweep, leading edge
AR	aspect ratio
BPR	bypass ratio
cg	center of gravity
DOC	direct operating cost
EDM	electro-discharge machining
EPNdB	effective perceived noise - dB

FAA	Federal Aviation Administration
FAR	Federal Aviation Regulation
FOD	foreign object damage
LFC	laminar flow control
OWE	operating weight empty
PL	payload
RSS	relaxed static stability
TOGW	takeoff gross weight

SCOPE

The study on which this paper is based has the following primary objectives:

- o Evaluation of alternatives in the design of LFC transports for operation in the 1990 time period.
- o Definition of requirements for subsystem development in subsequent program phases.

Figure 1 outlines the overall plan developed to achieve the study objectives. Using the projected technology data base and the selected study mission, a baseline configuration was developed. Concurrently, advanced LFC system concepts are being evaluated in the areas of:

- o Aerodynamics
- o Structures and materials
- o Suction systems
- o Leading-edge cleaning
- o Integration of auxiliary systems

As a part of the structures and materials task, a fabrication and test program for LFC surface elements culminates in the environmental and structural testing of .91 m x 1.52 m (3 ft x 5 ft) LFC surface panels. Upon completion of the concept evaluations and test programs, the optimum LFC system elements will be integrated into the baseline configuration as a part of the configuration selection and assessment task. The development of recommendations for subsequent activities will be based on the results of all study activities.

Although concept evaluations have been conducted in all appropriate technology areas, this paper will be limited to a description of the study baseline aircraft and a summary of progress in the design, fabrication, and testing of LFC surface panel components.

GUIDELINES

Mission Definition

An extensive evaluation of traffic projections and market analyses was conducted to define probable missions for commercial transports entering service in the post-1990 period. The selected mission is illustrated by the payload/range curve of figure 2. With a full passenger payload of 400, the study aircraft has a range of 12,038 km (6500 n mi) plus allowances for diversion to an alternate airport, winds at cruising altitude, track distances which exceed great circle distances, and a manufacturer's tolerance. The resulting still-air range is in excess of 13,890 km (7500 n mi) with full passenger payload. At reduced ranges, the aircraft has the capability of transporting the full passenger payload and 16,873 kg (37,200 lb) of belly cargo. Average stage length was estimated to be 6112 km (3300 n mi).

A cruise speed of $M = 0.80$ was selected for the study aircraft. Airport performance is compatible with projected international airports, with a FAR field length of 3048 m (10,000 ft) and maximum approach speed of 145 knots.

The market analysis established a minimum production quantity of 300 aircraft to be delivered over a 10-year period.

Reference Technology Levels

The assumed development schedule for the study aircraft is shown in figure 3. For initial passenger operation in 1993, the selected airframe and engine technology levels of 1988 and 1987, respectively, are appropriate. The technology levels illustrated in

figure 4 are consistent with the assumed development schedule for the study aircraft.

Aerodynamics

The level of aerodynamics technology considered in this study includes the use of advanced airfoil sections in the form of a modified supercritical airfoil. Favorable supercritical flow permits design of wings with low sweep and greater thickness. The baseline airfoil pressure distribution shown in figure 5 is a compromise between the high aft-loaded airfoil and the supercritical airfoil.

Flight Controls

Active controls are utilized to reduce wing bending moment on the wing to a level equivalent to a 2.0g symmetric maneuver without active controls. The use of trailing-edge wing active controls results in a wing torsion increase above the wing torsion loads for a 2.5g symmetric maneuver without active controls. The achievement of wing bending moment equivalent to a 2.0g maneuver is a 33% reduction in incremental bending moment. Torsion moment increases approximately 30%.

An active gust load alleviation is used to reduce wing bending due to gust on the inner 50% of the wing to the levels that would be obtained for a 2.0g symmetric maneuver without active controls. Gust loading is critical on this aircraft due to the high lift curve slope produced by the LFC and the high aspect ratio of the wing. A 40% - 50% reduction in incremental gust wing bending moment is required to achieve the desired load level. Wing torsion moment due to gust is low, and the active control system causes only a slight increase in torsion. This 40% - 50% reduction is obtained throughout the flight envelope with suitable wing and horizontal stabilizer trailing-edge control surfaces.

The aircraft is designed to be free from flutter and divergence at speeds up to $1.2 V_D/M_D$ in accordance with the requirements of paragraph 25.629 of FAR Part 25. Active flutter suppression is used to provide the flutter speed margin above V_D/M_D .

For the aircraft of this study, relaxed static stability (RSS) is employed to provide flexibility of establishing center-of-gravity envelopes. Assumptions for the RSS system employed for study aircraft are summarized below:

Aft cg limit (x/c)	0.51
Yaw acceleration control (rad/sec ²)	0.116
Pitch acceleration control (rad/sec ²)	0.265

In sizing the vertical and horizontal tails of study aircraft, adequate requirements were imposed for engine-out control, pitch acceleration capability, and yaw acceleration capability.



Propulsion

The Pratt & Whitney Aircraft STF-477 study engine was chosen as the basis for the primary propulsion units for the study aircraft. This engine cycle was the end product of Tasks II and III of a P&WA study performed under contract to the NASA Lewis Research Center and reported in reference 6.

The STF-477 twin-spool engine cycle has a fan pressure ratio of 1.7 at a bypass ratio of 8.0. The engine overall pressure ratio is 45 : 1 with a maximum combustor exit temperature of 1427°C (2600°F). The low-pressure spool consists of a one-stage fan and three low-pressure compressor stages. These components include advanced blading aerodynamics and seals for better component efficiency and lower noise while maintaining good component life and performance retention. The low-pressure spool is driven by a five-stage uncooled turbine, incorporating higher loading and advanced aerodynamics and seals. The high-pressure spool incorporates a ten-stage compressor driven by a two-stage highly-loaded turbine, both incorporating technology advances similar to the low-pressure spool. The high-pressure turbine also includes advanced metallurgy, cooling, and coating technologies.

Materials

The selection of materials for the major structural components of the study configurations was based on the results reported in the studies of references 5, 7, and 8. Candidate materials and structural concepts were examined for each element of the structure. Materials and concepts were selected on the basis of the lowest cost per pound of weight saved. Weight technology factors were developed for a constant-size airplane by substituting different materials and structural concepts and computing the weights of structural elements for identical structural requirements. A weight factor of 1.00 was assigned to the conventional aluminum structure, and the ratio of the advanced material and concept to that of aluminum was defined as the weight technology factor. The full benefits of advanced materials were realized by sizing the total airplane, including the power plant and other systems, to take advantage of the lower structural weights.

Table I describes the distribution of advanced materials among the airframe components and lists the corresponding weight technology factors. Utilization of advanced materials for 66% of the airframe weight results in study aircraft which weigh about 67% as much as comparable current transports.

Design Criteria

Recent projections of the IATA Technical Committee indicate that airlines will expect a minimum design life objective of 90,000 flight hours for long-range aircraft entering service in the post-1990 period. The airlines do not expect a crack-free structure for this length of service but do expect an airframe which can be maintained economically. Previous wide-body jet experience indicates that the airlines will expect a service life

warranty contract of approximately one-half of the design life objective. Therefore, a warranty service life of 45,000 flight hours was used to establish the wing ultimate tension cutoff stress level for the baseline airplane. The current wide-body jet warranty life is on the order of 30,000 flight hours.

The study aircraft satisfy the requirements for type certification in the transport category under Federal Aviation Regulations - Part 25, and are capable of operating under pertinent FAA rules.

Based on realistic estimates of achievable progress for the technology readiness date assumed for the study aircraft, the following noise criteria were selected:

- o Takeoff sideline FAR 36 -10 EPNdB
- o Takeoff flyover FAR 36 -6 EPNdB
- o Approach flyover FAR 36 -5 EPNdB

These levels are 2 EPNdB below the standards currently proposed as a part of NPRM 75-37C in reference 9.

The study aircraft are provided with fuel reserves in accordance with the requirements of FAR 121.645. In addition to the fuel reserve allowances specified in this regulation, the LFC study aircraft are designed with adequate reserve fuel to accommodate loss of the LFC system due to weather phenomena during six percent of the mission cruise time.

The basic design criteria for LFC systems developed as a part of the X-21 Program represent the most comprehensive set of guidelines currently available. Therefore, the criteria established by this program and reported in reference 10 form the basis for the definition of LFC systems for the study aircraft.

Elements of the LFC systems developed for study aircraft reflect advances in all technical disciplines which are appropriate for commercial aircraft to be introduced in the early-1990 period.

BASELINE CONFIGURATION SELECTION

Configuration Parameters

A comprehensive analysis was conducted to evaluate the influence of aircraft performance and geometry parameters on the economic efficiency of commercial transport aircraft compatible with the study mission. A conventional wide-body fuselage configuration, sized for 400 passengers and 16,873 kg (37,200 lb) of belly cargo, was used for all analyses. The parametric configurations use two LFC suction units mounted in the fuselage

near the wing root. Power for these suction units is independent of the main propulsion units and suction air is exhausted at free-stream velocity.

The results of the studies reported in reference 5 relative to the use of external fuel tanks, alternate engine locations, extent of laminarization, and various levels of static stability were used in design decisions for the baseline configuration.

The methodology employed in selecting configuration parameters is summarized in figures 6 and 7. A parametric configuration was optimized for each of the twelve cruise-altitude/cruise-M combinations shown in figure 6. The resultant aircraft were evaluated on the basis of direct operating cost. Optimum configuration parameters were developed for each combination using the procedure illustrated in figure 7. The optimization required two phases. In the first phase, wing loading and aspect ratio were varied to establish optimum configuration geometry independent of airport performance constraints. In the second phase, engine bypass ratio, cruise power ratio, and aspect ratio were varied parametrically to optimize airport performance for each configuration geometry.

The results of these analyses are summarized by figure 8, in which DOC is plotted versus cruise Mach number for the several altitudes considered. One additional optimization was also performed for a cruise altitude of 12,802 m (42,000 ft) to furnish more complete data for variation of DOC with altitude. The curves show that, between $M=0.75$ and $M=0.85$, DOC varies less than 0.018 ¢/seat km (0.03 ¢/seat s mi) for the two lowest altitudes. The leading-edge sweep angle of 0.437 rad (25 deg) associated with $M=0.80$ is less critical from a leading-edge contamination standpoint than the sweep of 0.551 rad (31.5 deg) associated with $M=0.85$. For this reason and others associated with the more severe design problems associated with compressibility effects, a cruise M of 0.80 was selected for the baseline aircraft.

As illustrated by the cross plot for $M=0.80$ shown in figure 9, higher altitudes suffer progressively greater DOC penalties. Since the lower unit Reynolds number associated with increasing altitude is beneficial to LFC because of its influence in reducing sensitivity to surface imperfections, an altitude of 12,192 m (40,000 ft) was selected as a reasonable compromise for the cruise altitude of the baseline aircraft.

Configuration Description

The general arrangement of the baseline aircraft selected to satisfy the previously defined mission requirements is illustrated in figure 10. The aircraft is a wide-body configuration designed to carry 402 passengers and baggage over an intercontinental range of 12,038 km (6500 n mi) at $M=0.80$ with adequate fuel to account for adverse winds, intermittent LFC disruptions due to atmospheric conditions at cruise altitude, and normal international fuel reserves. A typical cabin arrangement accommodates a 10/90 passenger mix, with 40 in first class and 362 in tourist class cabins. Space allowances are made for galleys, lavatories, closets, cabin crew provisions, as well as rest areas for flight crew as

dictated by FAR Part 121.485 for flights of more than 12 hours duration. Space for LD-3 cargo containers is provided forward of the wing box and aft of the main landing gear bay. A bulk cargo bay is also provided at the rear of the pressurized belly. These cargo bays will accommodate 16,873 kg (37,200 lb) of cargo.

The baseline airplane is a low-wing, T-tail, monoplane with four aft-fuselage mounted propulsion engines. An independently-driven LFC suction unit is located in a fairing under each wing root, as shown in figure 11. Fuel is carried in the wing including the wing center section box. The wing has a moderate sweep of 0.437 rad (25 deg) at the leading edge with an aspect ratio of 11.6. Full-span flaps, including drooped ailerons, provide the required airport performance. Leading-edge high-lift devices are not required. Partial-span spoilers are incorporated as required. Small-chord secondary flaps, incorporated into the main flaps, provide upper surface pressure gradient and shock position control for off-design operation as well as serving as active controls to minimize structural requirements.

LFC suction capability is provided on both wing surfaces from 0 to 75% chord, and on the empennage from 0 to 65% chord. The LFC ducting and metering system is integrated into the aircraft wing structure. A combination anti-icing, anti-contamination system is incorporated in the leading-edge region.

The weights for the different airplane groups were calculated from statistical weight equations based on current transport aircraft. These weights were adjusted in the primary and secondary structural areas by applying the composite and advanced material weight technology factors shown in table I. Other adjustments to the aircraft weight such as LFC engines and ducts were estimated by methods developed specifically for these elements. The surface panel weights were calculated from design layouts. A weight statement for the baseline LFC airplane is presented in table II. Weights of LFC system elements are listed in table III. It will be observed that the total weight of the LFC system is less than 3.6% of the aircraft operating weight.

The relative performance of the study aircraft is illustrated by figure 12. Based on the data of reference 11, figure 12 shows the fuel efficiency of representative current commercial transports as a function of stage length. The corresponding curves for the study aircraft show that, for a full passenger payload, the LFC transport has a fuel efficiency at the design range which is over 2.5 times that of current commercial aircraft. For a combined passenger/cargo payload, the fuel efficiency at shorter stage lengths is about 1.8 times that of current wide-body transports.

LFC Systems

The LFC system includes all portions of the boundary layer suction system, including the suction surface through which a portion of the boundary layer is taken into the airplane, the system for metering the level and distribution of the ingested flow, the ducting

system for collecting the flow, and the pumping units which provide the suction and sufficient compression to discharge the suction flow at velocity equal to or higher than free-stream.

Figure 13 shows a flow map of the LFC suction airflow for the complete aircraft. LFC flow is drawn forward at intervals over the wing through chordwise ducts into leading-edge trunk ducts which carry the flow inboard to the suction pumps. Empennage suction flow is carried from the tail surfaces through trunk ducts located in the fuselage to mix with wing flow prior to entry into the suction pumps.

Figure 14 depicts in some detail the selected LFC surface configuration with suction flow denoted by arrows. Boundary layer air is pulled through spanwise surface slots into spanwise capillaries, then through metering holes into the structural hat stiffeners. Suction flow is carried spanwise until it reaches the chordwise collector duct, which is formed by hollow rib caps located on alternate ribs.

The LFC surface is constructed of graphite/epoxy. Each element is bonded in place with mechanical fasteners used at rib caps to facilitate wing assembly. The entire surface is covered by a sheet of 0.51 mm (.020 in) titanium. This LFC surface is designed to accommodate slot spacings of 5.08 and 7.62 cm (2 and 3 in) or multiples thereof.

Figure 15 provides a cross-sectional view of the wing leading edge and shows the hat-stiffened surface panels with the integrated surface slots and ducting. The removable nose cap is maintained at a constant leading-edge radius in the wing-root region and incorporates a system of chordwise suction slots with sub-surface compartments to control spanwise contamination and the rapidly changing pressure gradients existing over the extreme leading-edge surface region. The anti-icing, anti-contamination system incorporated in the leading-edge region consists of a porous band at the upper and lower limits of stagnation point excursion across the leading-edge dictated by varying angle of attack. Each porous band is approximately 2.54 cm (1 in) wide, fed by a pressure system which sprays the liquid into the airstream on both sides of the stagnation point forming a cloud through which the wing passes.

The slot configuration of the baseline system for the LFC surfaces in the wing-box region is defined by the following:

- o Slot spacing 15.24 cm (6 in)
- o Slot width 0.28 mm (0.011 in) outboard of wing break
 0.31 mm (0.012 in) inboard of wing break
- o Skin thickness at slot 0.51 mm (0.020 in) outboard of wing break
 1.27 mm (0.050 in) inboard of wing break

Figure 16 presents a schematic of the metering system and illustrates the primary structural composite skin with the slots of the bonded titanium surface centered on the slot

duct. Metering holes penetrate the composite skin and meter the flow from the slot duct into the composite hat-section structural stringers. Significant dimensions include the slot duct width, b , which is limited to 7.6 mm (0.30 in) by the allowable overhang of the 0.51 mm (0.020 in) thick titanium surface skin. The slot duct depth, h , is a selected value but should be held to a low value to minimize structural impact of the slot on the composite skin. The metering hole diameter, d , spacing, s , and offset, y , are selectable dimensions. It is advantageous to maintain a high offset value. Therefore offset is taken to be the maximum possible within the limits of metering hole tangency to the slot duct wall and the diameter of the metering hole.

The following summarizes the metering configuration selected for the wing-box region of the study aircraft:

- o Slot duct width, b 7.6 mm (0.30 in)
- o Slot duct depth, h 2.5 mm (0.10 in)
- o Metering hole diameter, d 2.1 mm (0.083 in)
- o Metering hole spacing, s 12.7 mm (0.50 in)

Figure 17 shows a schematic of the suction ducting system and illustrates the chord-wise flow of suction air forward to the trunk ducts and then inboard to the suction pumps. The low-pressure air from the upper wing surface and leading-edge region enters the forward trunk duct, while the high-pressure flow from the lower surface enters the aft duct. A shut-off valve is provided in both trunk ducts to isolate the inboard wing surface, thus permitting continued laminarization of this surface in the event of the failure of a suction pump. Shut-off valves are also provided in the pump inlet ducts to permit isolation of a failed pump and allow in-flight starting of the suction pump with ambient air by means of the ambient vent valves. The pressure in the duct system in-flight is always well below ambient and if this ambient vent arrangement were not provided, the pump would be required to start under load. Cross ducts are provided between the pump inlet ducts. The empennage suction flow is ducted into the low-pressure duct system through a shut-off valve.

The pump consists of a primary element with a boost element provided for the low-pressure flow. Pump discharge is turned through approximately 3.15 rad (180 deg) and discharged through a nozzle in a near axial direction at free-stream velocity. The pump is driven by an independent shaft engine provided with a ram inlet and a near axial discharge at free-stream velocity.

Calculated pressure losses are shown in table IV for the suction systems on the selected configuration. Accumulated pressure losses are shown as a percent of the static pressure acting on the surface of the airfoil. This does not allow for any pressure recovery due to the small velocity heads present in the boundary layer flow removed by the suction system. These accumulated losses are indicated for the entry and exit flow in each component of the ducting system. The pressure loss at the entry to the hat section includes

the losses associated with the slot and metering system. All losses include the accumulated duct, metering and mixing losses to that point in the system.

LFC SURFACE PANEL DEVELOPMENT

The overall plan employed for the development of LFC surfaces is outlined in figure 18. As illustrated by this flow diagram, the plan proceeds from the selection of a design concept through the development of detailed designs, the formulation of manufacturing procedures, and two phases of panel fabrication and testing prior to the ultimate definition of panel design criteria.

Panel Design

Following the conceptual design activities devoted to the identification of candidate concepts, preliminary design investigations were conducted to develop consistent weight and cost factors for comparison during the evaluation. To develop these data, the preliminary design effort included the estimation of loads for a typical LFC aircraft wing, selection of materials, and the sizing of various surface/wing elements. For study purposes, the evaluation was restricted to the portions of the LFC upper and lower surfaces forming the main structural elements between the wing front and rear spars.

In addition to the above, the following were accomplished for each design concept:

- o Manufacturing procedures were developed.
- o Estimates of manufacturing costs were completed.
- o Maintainability and reliability were assessed.
- o Procedures for repairing damaged surfaces were developed.
- o Compatibility with surface design criteria and other elements of the LFC system was evaluated.

Upon completion of this procedure for each of the candidate concepts, recommended non-structural, structural, and combination concepts were selected. These concepts were subsequently compared to permit selection of a single concept.

During the course of the evaluation, a total of four non-structural concepts, six structural concepts, and three combination concepts, employing elements of both non-structural and structural designs, were evaluated. On the basis of these evaluations, the skin and hat-section stiffener design illustrated in figures 14 and 15 was selected for further development.

Details of the surface concept, including the selection of materials and number and orientation of the 5208/T300 graphite/epoxy plies, are shown in figure 19. The selection of titanium for the face sheet was based on requirements for lightning protection and resistance to erosion and corrosion.

Manufacturing Procedures

The manufacturing procedures evaluated during this phase of the study were directed toward the development of two .91 m x 1.52 m (3 ft x 5 ft) LFC surface panels to be employed in subscale testing. To permit fabrication of the selected LFC surface design, manufacturing development was required to economically produce acceptable slots in titanium and fabricate basic hat-stiffened wing-box structure from graphite/epoxy composite material in sections thicker than had previously been fabricated. A variety of slotting procedures and graphite/epoxy structure fabrication and assembly procedures were evaluated in the selection of manufacturing procedures providing a high-quality, dimensionally accurate LFC wing panel structure. Following is a brief discussion of the investigations conducted.

Surface Slotting

The following criteria were established for slots in the titanium LFC surface:

- o A slot width range of 0.076 mm to 0.228 mm (0.003 to 0.009 in).
- o A slot width tolerance of $\pm 10\%$.
- o The slot entrance equal to or thinner than the slot exit to minimize slot contamination.
- o Sharp slot edges to facilitate control of air flow through the slots.

Table V summarizes the results of investigations conducted in the evaluation of candidate slotting procedures. Of the eight procedures evaluated, including both pre-assembly and post-assembly techniques, the electro-discharge machining (EDM) process was judged to be most compatible with requirements for the slotting of titanium in a production environment. However, initial results obtained with the laser are sufficiently promising that this procedure should be the subject of further investigation.

The EDM procedure results in a slot which is somewhat wider on the side of the sheet from which the cutting is accomplished. Consequently, due to the requirement that the slot entrance be equal to or smaller than the slot exit on the wing surface, it is necessary to slot the titanium skin prior to assembly. To facilitate handling of the skin during the slotting and bonding process, 1.27 mm (0.050 in) connecting tangs were left in the slots at 15.24 cm (6 in) intervals. After bonding, the tangs were removed with a jeweler's saw.

A photograph illustrating the EDM procedure is shown in figure 20.



Structural Skin

A major problem in the development of thick sections of 5208 graphite/epoxy was the ply thickness distribution through the skin. Bleeding from one side yielded plies against the bleeder which were too thin and plies away from the bleeder which were too thick. A 20-ply stack which was pre-bleed yielded uniform ply thickness. Thus, pre-bleed was selected as the preferred process for thick 5208 graphite/epoxy sections.

Slot ducts were formed by aluminum strips tack riveted to the skin tool with 16-ply graphite/epoxy between the aluminum strips. An aluminum foil backing sheet was used to prevent splintering during drilling of the metering holes. Figure 21 illustrates the completed structural skin.

Hat-Section Stiffeners

The hat-section stiffeners were produced in a female mold. A 0.61 m (24 in) long prototype tool was made from aluminum, and an attempt was made to let the vacuum bag mold the inside of the part. While the part was generally acceptable, there were wrinkles caused by bag folds. Cracking also occurred in the 20-ply 0° stacks in the hat crown. The four-ply (+45/-45/-45/+45) modules were pre-bleed prior to forming into the mold. Pre-bleed modules were found to be much easier to form since they were well compacted.

A rubber plug was made to mold the center of the hat and was used on additional prototype runs. Cracking of the 0° plies in the crown was not resolved. One try placed a ply of graphite fabric in the center of each of the 20-ply 0° stacks but failed to alleviate the cracking. Some changes to the cure cycle were also made, but neither helped the cracking problem or completely eliminated voids. Crack-free structural components were achieved by reducing the number of 0° plies in the crown to ten. Completed hat-section stiffeners are shown in the photograph of figure 22.

Panel Assembly

In the bonding of the hat-section stiffeners to the structural skin, the web flange stiffness of the hat sections was found to be adequate to withstand light autoclave pressure. Therefore, a verification bond run with the adhesive encapsulated in 0.013 mm (0.0005 in) Teflon was conducted at 68.94 kN/m² and 137.88 kN/m² (10 psi and 20 psi) autoclave pressure. After the adhesive cured, the hat was stripped from the skin and a replica of the bond line was removed from between the Teflon. Both cure pressures produced a good bond with adhesive thickness from 0.051 mm to 0.152 mm (.002 in to .006 in).

In bonding the titanium skin to the structural skin, the initial attempt used a 121°C (250°F) curing adhesive, American Cyanamid FM 73. A demonstration panel was made by bonding a strip of slotted titanium to a part of the first 96-ply panel. Warpage of 1.01 mm (.040 in) in 0.61 m (24 in) was experienced, which precluded using an elevated temperature bonding procedure for attaching the titanium skin to the surface panel. A room-

temperature curing adhesive was selected which had been used previously for bonding titanium doublers to aluminum structure on aircraft. Both Hysol EA 9309.1 and MIL-S-8802 polysulfide sealant were evaluated as room-temperature curing adhesives. The panel with MIL-S-8802 resulted in non-uniform bond lines and a step at the slot edges; therefore, Hysol EA 9309.1 was selected. This adhesive, made by the Hysol Division of the Dexter Corporation, is a two-component paste and can be used under vacuum pressure applications. A demonstration panel was made and exhibited no warpage.

A photograph of the panel during assembly is presented in figure 23. The completed surface panel is shown in figure 24. Table VI compares LFC surface smoothness criteria and the values achieved on this panel.

Summary of Manufacturing Procedures

The following summarizes the manufacturing procedures employed for fabrication of the first two LFC surface panels:

- o The outer skin, inner skin, and hat stiffeners are separately cured and subsequently joined by structural adhesive bonding. During the final bonding cycle, the shear clips are integrally molded in place.
- o The titanium face sheet is slotted using the electro-discharge machining process. In this process, 1.27 mm (0.050 in) tangs are left in the slots at 15.24 cm (6 in) intervals to maintain integrity of the sheet and permit handling prior to final assembly.
- o The slotted face sheet is bonded to the outer skin with room-temperature curing adhesive and the tangs are removed with a jeweler's saw.

Subsequent testing of surface panel components showed the selected manufacturing procedures to be satisfactory with two exceptions:

- o In many cases, slot width tolerances were exceeded in the removal of connecting tangs. Alternatives to the use of hand-held jewelers' saws are being investigated.
- o In compression testing of the panel, the titanium skin began buckling and disbonding at approximately 50% of the failure load. The room-temperature curing adhesive used for this bond will be replaced with an adhesive that cures at an elevated temperature. Identification of a suitable adhesive is currently in progress.

Panel Testing

Subscale testing of LFC surface panels was conducted in the following areas:



Environmental

- o Temperature
- o Icing
- o Corrosion
- o Foreign object damage
- o Repairability
- o Lightning

Structural component tests

- o Rib clip tension
- o Rib clip shear
- o Compression

Test specimens were cut from the two .91 m x 1.52 m (3 ft x 5 ft) LFC surface panels described in the preceding section. A photograph of the first surface panel illustrating the allocation of test specimens is presented in figure 25. The sectioning of the second surface panel to acquire the large specimens for the compression tests is illustrated by figure 26. The number and characteristics of test specimens is outlined in table VII. The narrative which follows summarizes pertinent results of selected tests.

Temperature

Thermal testing was conducted to evaluate the effect of temperature changes on the width of slots in the LFC surface panel and to verify handbook values for the thermal coefficient of expansion for the thick composite structural skin. The thermal test panel and instrumentation are illustrated by figure 27. In the temperature range from -51°C (-60°F) to 82°C (180°F), the maximum variation in slot width ranged from $+6.35$ and -6.10×10^{-4} mm ($+25$ and -24×10^{-6} in). Thus, slot width variations due to temperature changes are considered to be insignificant. An acceptable comparison of measured and handbook values for the coefficient of expansion for the composite structure was obtained.

Icing

Icing tests were conducted to evaluate the effect of entrapped water in the hat-section stiffeners and in the surface ducts and metering holes.

As shown by figure 25, a specimen was cut from the panel for icing tests, and the ends of the hats were closed by clamping aluminum plates with a rubber seal to each end. A stand-pipe was attached to one end and filled with water. The specimen was placed in a low-temperature chamber and frozen at -18°C (0°F). One hat flange separated from the skin. As illustrated by figure 28, failure was within the composite hat flange. The flange separation emphasizes the need to keep water out of the hat sections during low-temperature operation.

For the evaluation of icing in the surface ducts and metering holes, the ducts and holes were filled with water through the skin slots. The specimen was exposed to 15 freeze-thaw cycles. There was no visually detectable damage after the 15 freeze-thaw cycles. Removal of the titanium skin did not reveal any hidden damage. A section was cut through a metering hole, and the specimen was mounted and polished. Microscopic examination up to 200X showed no delamination or cracking.

Corrosion

Tests were conducted to evaluate the effect of environments representative of those encountered in airline operations on the bending strength of the LFC surface panel.

Three 10.16 x 25.40 cm (4 x 10 in) panel specimens were exposed to 30 days of salt fog, 30 days of high humidity, and 30 days of Weather-O-Meter, respectively. In addition, a 0.15 x 0.61 m (6 x 24 in) specimen was exposed to 30 days in the Weather-O-Meter environment. After exposure, the specimens were static tested in a four-point bending test, as illustrated by figure 29. Test results are summarized in table VIII. As shown in table VIII, the maximum reduction in bending strength was 18% for the specimen subjected to the Weather-O-Meter environment.

Foreign Object Damage

The objective of this test was to determine the resistance of an LFC surface panel to foreign object damage.

Using the experimental arrangement shown in figure 30, the LFC surface panel was impacted over the slotted surface duct and over the composite-supported titanium at energy levels of 5.76, 11.52, 23.04, 46.08, and 92.16 m-kg (5, 10, 20, 40, and 80 in-lb). The depth of the maximum indentation at each impact point was measured with a depth micrometer and is reported in table IX. Figure 31 shows the result of a 92.16 m-kg (80 in-lb) impact over a surface duct. Apparent damage over solid laminate supported titanium was minimal. Removal of the titanium skin revealed little visual damage to the composite over the plenum and none over solid laminate.

The data of table IX indicate that none of the impacts in the range tested would create a surface indentation sufficiently deep to cause transition of the laminar boundary layer if the impact occurred over titanium supported by composite. However, depending on chord location, impacts in the range of 11.52 - 23.04 m-kg (10 - 20 in-lb) over a surface plenum would result in an unacceptable surface discontinuity. For purposes of comparison, a 1.27 cm (0.5 in) diameter stone at a relative velocity of 120 K is equivalent to a 57.6 m-kg (50 in-lb) impact energy level.



Repairability

The objective of this investigation was to demonstrate that typical damage to the slotted titanium LFC surface can be repaired by methods usable in-service by fleet operators.

The LFC surface panel specimen which was damaged in the foreign object damage test described in the preceding section was used as the test specimen. Repairs were made to the dents produced by the 23.04 m-kg (20 in-lb) to 92.16 m-kg (80 in-lb) impacts in the titanium over the surface ducts.

Removal of the damaged titanium surface with a hole saw was considered to be partially successful. A pilot hole was drilled in the center of the damaged area and allowed to penetrate the composite for approximately 0.63 cm (0.25 in). Additional control of the cutting tool was accomplished with a guide. Removal of the titanium skin was readily accomplished with the hole saw but it was not possible to stop the cut precisely in the adhesive layer and slight scoring of the composite occurred each time.

The second method attempted was the use of a counterbore, chucked in a low-speed, hand-held, drill motor. A pilot hole and cutting guide were used. The cut was terminated in the adhesive layer with no damage to the composite substrate. No problem was experienced with overheating. However, the edge of the cut in the titanium was not square due to the normal radius on a counterbore. A special counterbore was prepared with a square edge and a grind more suited to titanium cutting. Excellent results were obtained. Control of the cut using the hand-held drill was easily accomplished.

A patch was prepared from EDM-slotted titanium sheet with a connecting tang in the center of the patch, as illustrated by figure 32. Preparation for bonding was by conventional procedures. The composite surface was prepared by light sanding followed by an acetone wash. Both surfaces were lightly coated with Hysol EA 9309 adhesive and the patch was placed in position. Small strips of shim stock were used to align the slots, light pressure was applied, and the adhesive was allowed to cure at room temperature. The connecting tang was removed using a hand-held jeweler's saw.

Step profile measurements were made on several patches to determine smoothness. A typical patch had a total surface variation within a 5.08 cm (2 in) circle of only 0.063 mm (0.0025 in) and a maximum step of 0.038 mm (0.0015 in), which is well within the requirements established in reference 5.

It was demonstrated that a damaged slot can be returned to the original configuration using hand-held tools. While the tests were conducted on a bench, the entire operation could have been conducted either on the upper or lower surface of an aircraft wing. Repairs of this nature could be performed within a time span of four to six hours by using heat lamps to accelerate the adhesive cure.

Lightning

Preliminary tests were performed to ensure that the structural arrangement of the LFC surface panel is resistant to lightning strike. The test specimen shown in figure 25 was tested by NASA personnel in the NASA LRC lightning strike test facility.

Two specimens were tested. One panel was tested for baseline data and the other was subjected to 260 thermal-humidity cycles. Test conditions are outlined in table X.

In all six tests, the titanium face sheet was effective in preventing the current from penetrating the composite. The panel after four lightning strikes is shown in figure 33. The extent of disbonding between the face sheets and composite was examined using ultrasonic techniques. The results of this effort and the physical appearance of the panels suggest the possibility that aerodynamic forces encountered after a lightning strike might cause additional delamination. Indeed, these aerodynamic forces might become more intense due to irregularities in the wing surface caused by the lightning strike and the subsequent loss of local laminar flow.

The LFC panel used for these tests incorporated no underlying metallic structure or wiring. It is important to point out that the introduction of such conductors might alter the extent to which lightning current would tend to enter the composite structure. Such common elements as rivets, rib clips, and wiring bundles could cause intensification and internal arcing. These tests did, however, establish that lightning strikes to wing panels would not cause a catastrophic bond failure.

Compression

The objective of the panel compression test was to obtain design data for a four-element compression panel. The acceptable criterion for the compression panel was a design ultimate load of 6.49 MN/m (37.08 kips/in) without failure.

A 0.61 m x 1.52 m (24 in x 60 in) compression panel was removed from the second LFC wing surface panel shown in figure 26. The specimen ends were potted using Magnabond 69-9 tooling plastic and machined as required for the test configuration. The specimen was instrumented with thirty-four axial strain gauges and seventeen deflection transducers. Aluminum "T" sections, simulating rib caps, were attached to the rib clips.

The compression test of the four-element panel was conducted in a 5.34 MN (1200 kip) Baldwin Universal Testing Machine. The 5.34 MN (1,200,000 lb) load range was used, having an accuracy of plus or minus 0.5 percent of indicated load. All strain gauge and deflection transducer readings were recorded by a B&F Model SY 156 data acquisition system.

The specimen was loaded in .445 MN (100,000 lb) increments. While loading between .890 MN (200,000 lb) and 1.334 MN (300,000 lb), it was noted that the titanium



skin was buckling at the top and the bottom edge of the panel, including areas that had previously been determined to have some disbonding. This was documented by the photograph shown in figure 34. Loading was continued to 2.224 MN (500,000 lb) and buckling of the titanium strips progressed over the length of the panel, as shown in figure 35. The specimen withstood 3.959 MN (890,000 lb), the design ultimate load, when failure occurred by delamination of the hats and skin, as shown in figure 36.

Following is a summary of significant events during the test:

<u>MN</u>	<u>Load</u> <u>1000 lb</u>	<u>Maximum</u> <u>strain</u>	<u>Equivalent G</u> <u>force</u>	
.890	200	.0012	.84	Audible noises
1.334	300	.0019	1.26	Titanium skin began buckling
2.224	890	.007*	3.75	Panel failed at 100% ultimate load

* Extrapolated value. No strain data were obtained at failure.

Both the environmental testing and the structural testing conducted in this phase of the study provided results demonstrating the compatibility of the selected LFC surface panel design with the anticipated operational environment for future LFC transports.

CONCLUDING REMARKS

This paper has illustrated some selected aspects of the development of a practical LFC configuration for the 1990's and provided some insight into the development of an efficient LFC wing design. Current study results support the following conclusions:

- o The optimum performance and geometry parameters for a commercial transport utilizing LFC are not appreciably different from those for current turbulent transports. The selection of a cruise Mach number of 0.80 and a cruise altitude of 12,192 m (40,000 ft) provides near-minimum DOC and permits reasonably efficient LFC system design.
- o The most efficient LFC wing design is one which integrates the LFC ducting and metering system into advanced composite wing structure.
- o Although all surface smoothness requirements were not satisfied in all areas of the two LFC surface panels fabricated to date, it appears that additional manufacturing development will permit the fabrication

of graphite/epoxy structural elements with a slotted titanium surface which will be compatible with LFC system requirements.

- o Environmental and structural testing have illustrated the requirement for relatively minor changes in panel design and manufacturing procedures. Testing to date has verified the compatibility of the selected panel design and the use of composite materials with the requirements of LFC wing surface panels.

Although they are not described in this paper, parallel efforts are proceeding in the analysis of the laminar boundary layer, optimization of LFC airfoil and wing designs, the evaluation of alternative LFC system elements, and the evaluation of concepts to prevent leading-edge contamination. The results of these activities will contribute to the data base requisite to the ultimate validation of LFC in an operational environment.

REFERENCES

1. Antonatos, P. P.: Laminar Flow Control Concepts. *Astronautics and Aeronautics*, July, 1966.
2. Whites, R. C., Sudderth, R. W., and Wheldon, W. G.: Flight Test Results of the Laminar Flow Control X-21 Airplane. *Astronautics and Aeronautics*, July, 1966.
3. Anon.: Division Advisory Group Review - X-21A Program Summary. DAG 65-1-0, Northrop Corporation, Norair Division, 1965.
4. Anon.: Report of Review Group on X-21A Laminar Flow Control Program. USAF Aeronautical Systems Division, November, 1965.
5. Sturgeon, R. F., et al: Study of the Application of Advanced Technologies to Laminar-Flow Control Systems for Subsonic Transports. Vol. II, NASA CR-133949, prepared by the Lockheed-Georgia Company under Contract NAS1-13694, May, 1976.
6. Gray, D. E., et al: Study of Turbofan Engines Designed for Low Energy Consumption. PWA-5318, NASA CR-135002, Pratt & Whitney Aircraft Div. of United Technologies Corp., April, 1976.
7. Lange, R. H., et al: Study of the Application of Advanced Technologies to Long-Range Transport Aircraft. Vol. I, NASA CR-112088, prepared by the Lockheed-Georgia Company under Contract NAS1-10701, May, 1972.
8. Boundary Layer Control Study, Oral Status Report, prepared by the Boeing Company under USAF Contract F33615-76-C-3035, July, 1976.

9. NPRM 75-37C, "Noise Standards, Aircraft Type and Airworthiness Certification. Proposed Alternative Noise Reduction Stages and Acoustical Change Requirements for Subsonic Transport Category Large Airplanes, for Subsonic Turbojet Powered Airplanes and for Single Engine Transport Category Airplanes," Federal Register, Vol. 41 No. 209, Oct. 28, 1976.
10. Staff, LFC Engineering Section: Final Report on LFC Aircraft Design Data, Laminar Flow Control Demonstration Program. NOR 67-136, Northrop Corporation, Norair Division, June, 1976.
11. Shevell, R. S.: Technology, Efficiency, and Future Transport Aircraft. Astronautics and Aeronautics, September, 1975.

TABLE I. - WEIGHT TECHNOLOGY FACTORS

<u>Component</u>	<u>Advanced material weight (%)</u>	<u>Weight technology factor</u>
Wing	85	0.61
Fuselage	71	0.66
Horizontal tail	67	0.74
Vertical tail	67	0.74
Nacelle and pylon	35	0.79
Landing gear	23	0.84
Weighted average	66	0.67

TABLE II. - WEIGHT SUMMARY

	<u>kg</u>	<u>lb</u>
Structure	64,320	141,808
Propulsion system	15,585	34,359
Systems and equipment	30,138	66,441
Weight empty	(110,043)	(242,608)
Operating equipment	14,007	30,880
Operating weight empty	(124,050)	(273,488)
Passenger payload	38,465	84,800
Zero fuel	(162,515)	(358,288)
Fuel	94,654	208,673
Gross	257,169	566,961

TABLE III. - LFC SYSTEM WEIGHTS

	<u>kg</u>	<u>lb</u>
Surfaces		
Wing	2077	4578
Horizontal tail	197	435
Vertical tail	240	528
Suction units	489	1079
Ducting	854	1883
Installation	<u>607</u>	<u>1338</u>
Total	4464	9841

TABLE IV. - REPRESENTATIVE SUCTION SYSTEM PRESSURE LOSS

<u>Suction flow station</u>	<u>Cumulative pressure loss % P/H_s</u>
Wing surface	0
Spanwise hat section duct:	
Entering	1.07
Leaving	1.10
Chordwise ducts:	
Entering	1.85
Leaving	5.00
Trunk duct:	
Tip	8.50
Root	9.00
Pump inlet	10.00

TABLE V. - EVALUATION OF SLOTTING PROCEDURES

	<u>Verified production potential</u>	<u>Comments</u>
Electro-discharge machining	Yes	Further development required to get slot width to 0.076 mm (0.003 in)
Joining machined strips		
Bonding	No	Slot tolerance exceeded 0.025 mm (\pm .001 in)
Welding	No	Slot tolerance exceeded 0.025 mm (\pm .001 in)
Electron beam	No	Failed to produce slots consistently
Water jet	No	Too slow in titanium
Laser	To be determined	
Planer	No	Minimum slot width of 0.20 mm (0.008 in)
Saw	No	Too slow in titanium
Chem-milling	No	Failed to provide square corner

TABLE VI. - SURFACE TOLERANCE COMPARISONS

	Tolerance		Measured values			
	<u>mm</u>	<u>in</u>	<u>No.</u>	<u>No. exceeding</u>	<u>Maximum</u>	
					<u>mm</u>	<u>in</u>
Steps	0.152	0.006	60	1	0.161	0.0063
Waves (5.08 cm, 2 in)	0.076	0.003	60	11	0.114	0.0045
Slot width (Nominal 0.152 mm, 0.006 in)	0.015	0.0006	207	37	0.051	0.002

TABLE VII. - TEST SPECIMENS

<u>Type of test</u>	<u>Number of specimens</u>	<u>Dimensions</u>	
		<u>cm</u>	<u>in</u>
Temperature	1	30.5 x 91.4	12 x 36
Icing	1	15.2 x 30.5	6 x 24
Corrosion (4 pt bending)			
Skin	4	10.2 x 25.4	4 x 10
Panel	2	15.2 x 61.0	6 x 24
Foreign object damage and repairability	1	30.5 x 30.5	12 x 12
Lightning (6 strikes)	2	30.5 x 30.5	12 x 12
Rib clip			
Tension	1	15.2 x 30.5	6 x 12
Shear	1	15.2 x 30.5	6 x 12
Compression			
2 elements	1	30.5 x 91.4	12 x 36
4 elements	1	61.0 x 152	24 x 60

TABLE VIII. - TEST SUMMARY - CORROSION/BENDING

<u>Environment</u>	<u>Specimen</u>		<u>Reduction in bending strength - %</u>
	<u>cm</u>	<u>in</u>	
Salt fog	10.2 x 25.4	4 x 10	11
Humidity	10.2 x 25.4	4 x 10	13
Weather-O-Meter	10.2 x 25.4	4 x 10	18
Weather-O-Meter	15.2 x 30.5	6 x 24	7

TABLE IX. - TEST SUMMARY - FOREIGN OBJECT DAMAGE

<u>Impact load</u>		<u>Over duct</u>		<u>Over laminate</u>		<u>Ply damage</u>
<u>m-kg</u>	<u>in-lb</u>	<u>mm</u>	<u>in</u>	<u>mm</u>	<u>in</u>	
5.76	5	0.025	0.001		0	0
11.52	10	0.152	0.006	0.025	0.001	0
23.04	20	0.457	0.018	0.050	0.002	0
46.08	40	0.508	0.020	0.075	0.003	0
92.16	80	0.813	0.032	0.101	0.004	10



TABLE X. - TEST RESULTS - LIGHTNING STRIKE

<u>Test number</u>	<u>High voltage spike kV</u>	<u>Continuing current</u>		<u>Edges grounded</u>	<u>Burn thru</u>	<u>Disbond</u>
		<u>amp</u>	<u>msec</u>			
1	25	0	0	All	No	No
2	42.5	0	0	All	No	Some
3	25	500	200	All	Yes	Yes
4	25	500	200	One	Yes	Yes
5	25	500	200	All	Yes	Yes
6	45	0	0	All	No	Yes

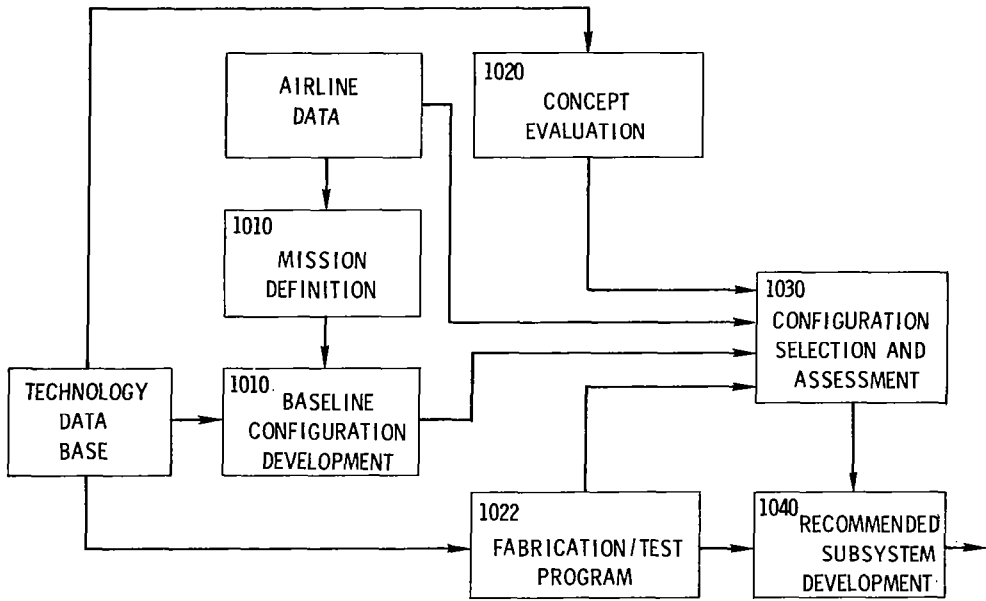


Figure 1.- Study plan.

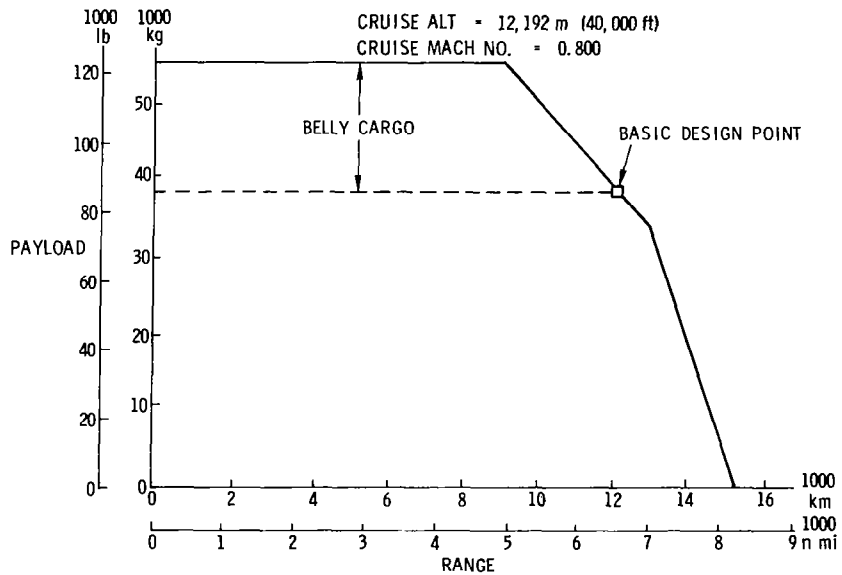


Figure 2.- Payload/range.

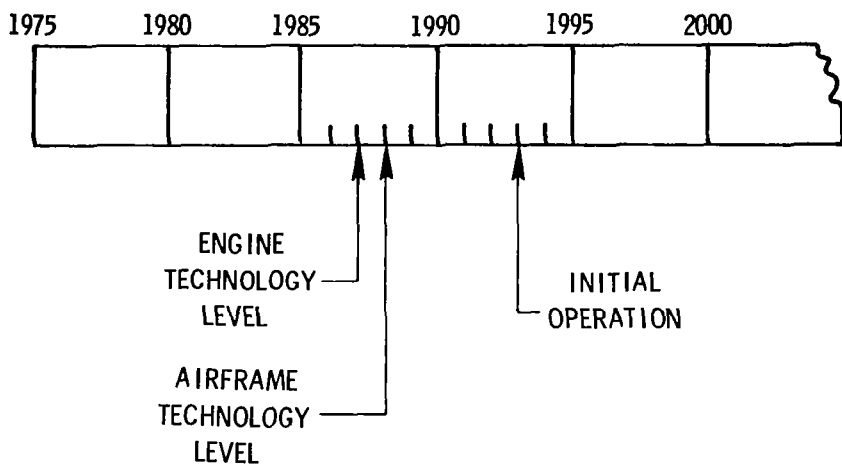


Figure 3.- Development schedule.

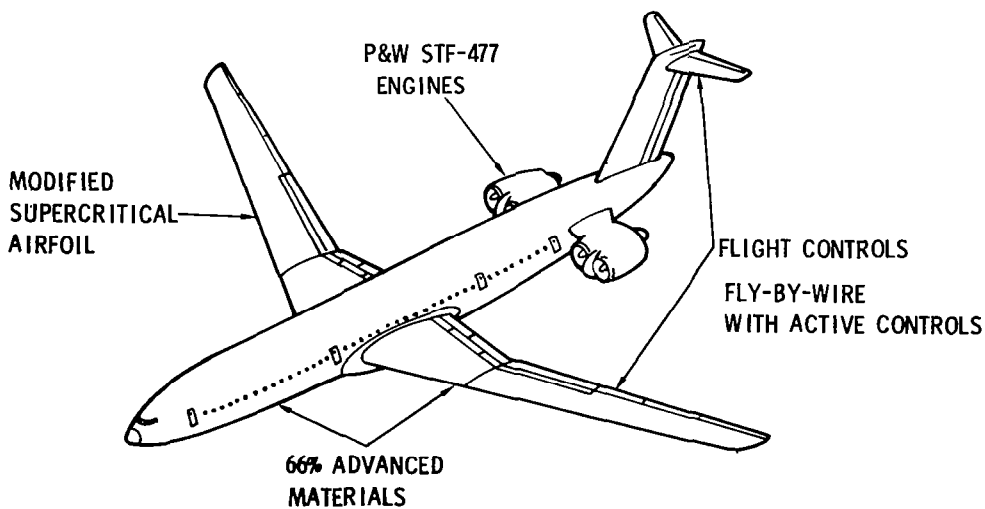


Figure 4.- Reference technology level.

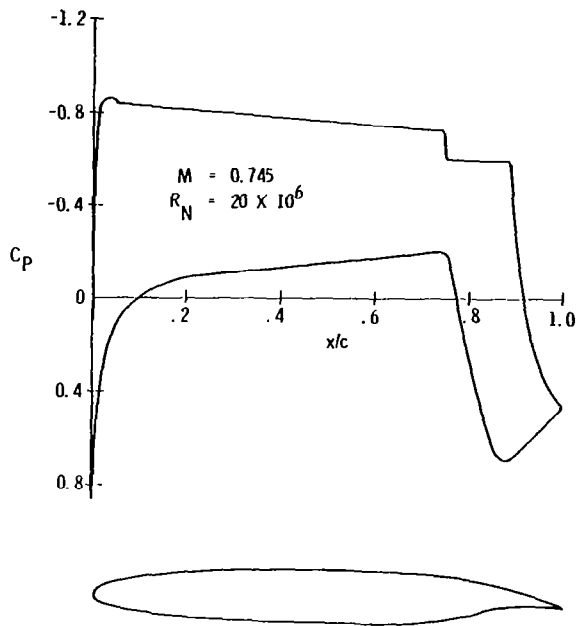


Figure 5.- Airfoil design pressure distribution.

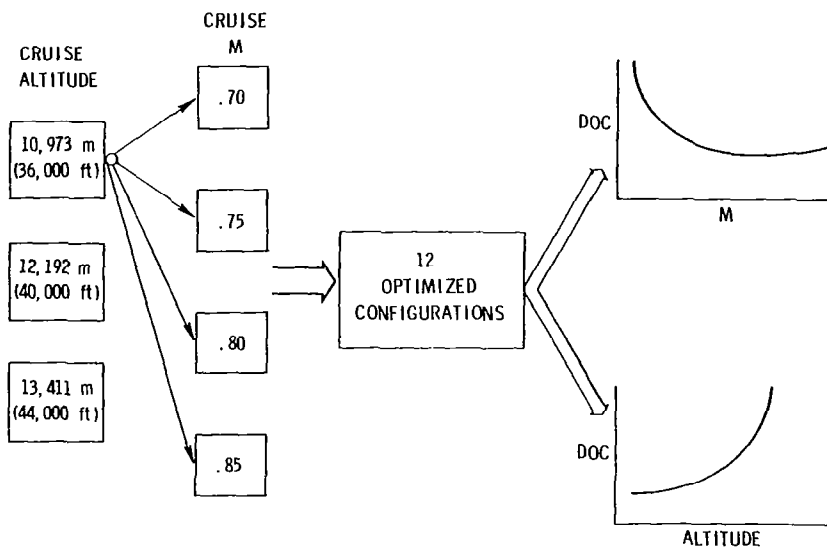


Figure 6.- Parametric configurations.

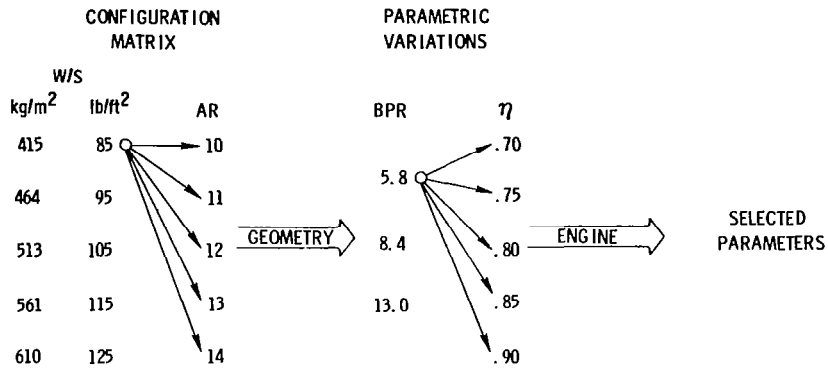


Figure 7.- Parametric procedures.

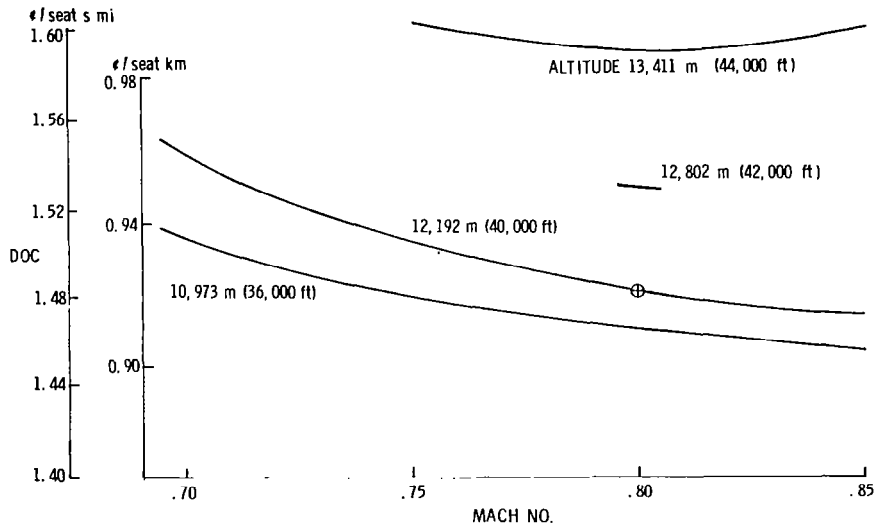


Figure 8.- Variation of DOC with Mach number.

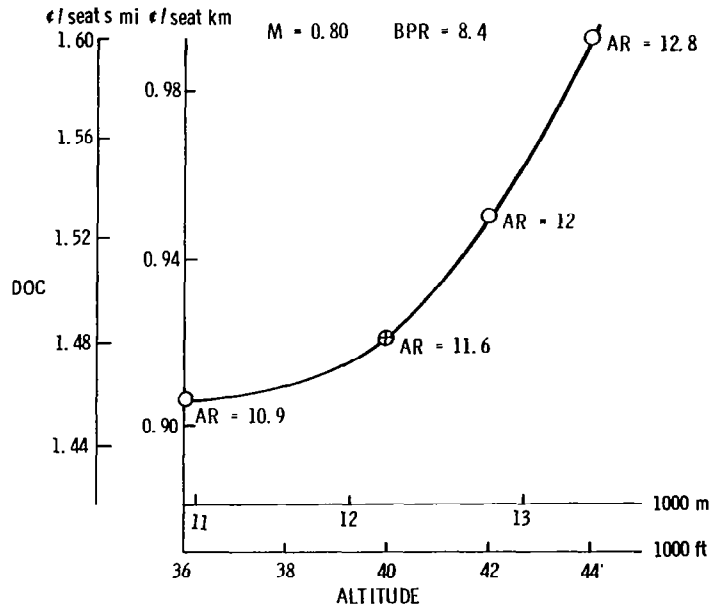


Figure 9.- Variation of DOC with altitude.

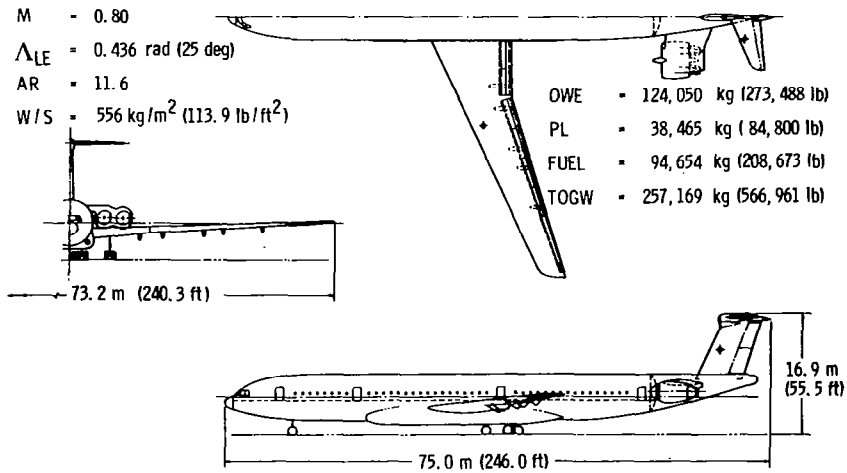


Figure 10.- Baseline aircraft configuration.

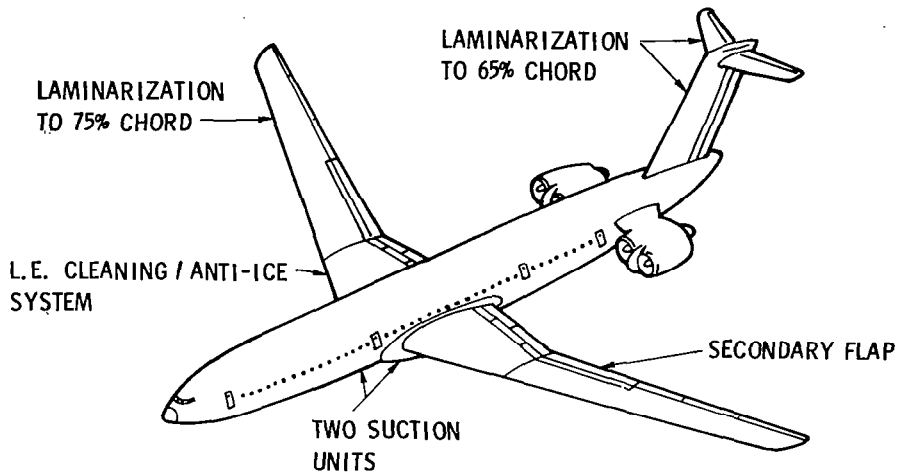


Figure 11.- LFC system configuration.

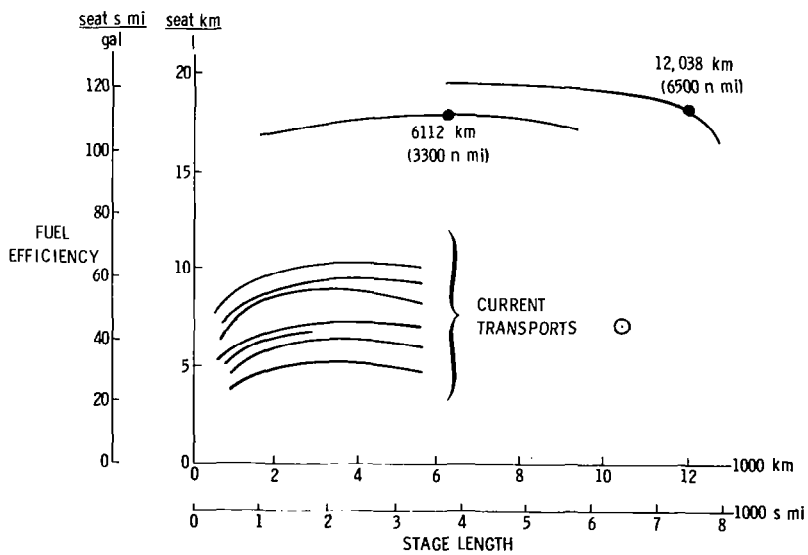


Figure 12.- Fuel efficiency comparison.

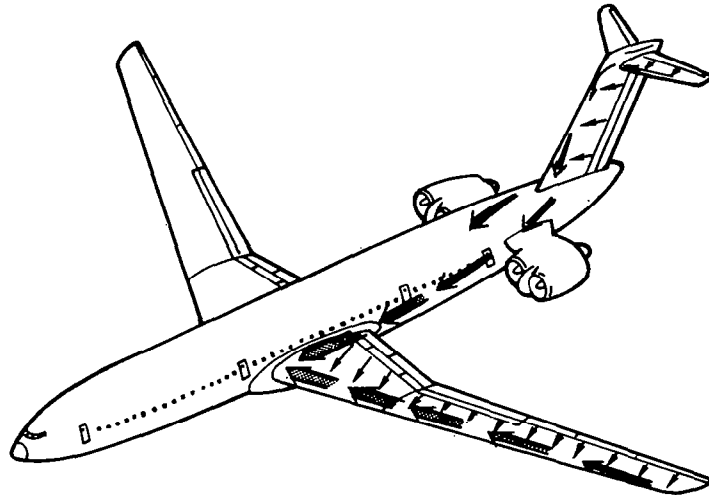


Figure 13.- LFC ducting configuration.

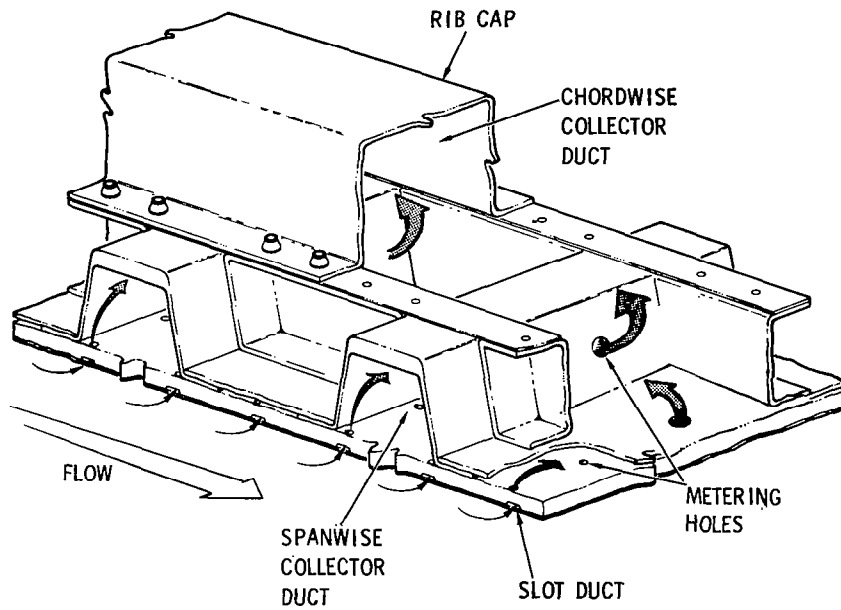


Figure 14.- LFC surface design.



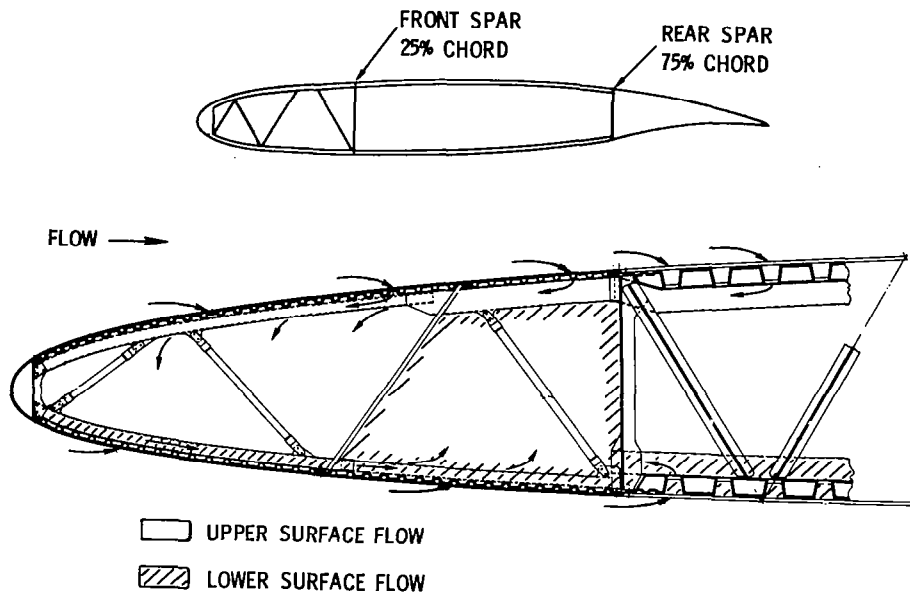


Figure 15.- LFC wing design.

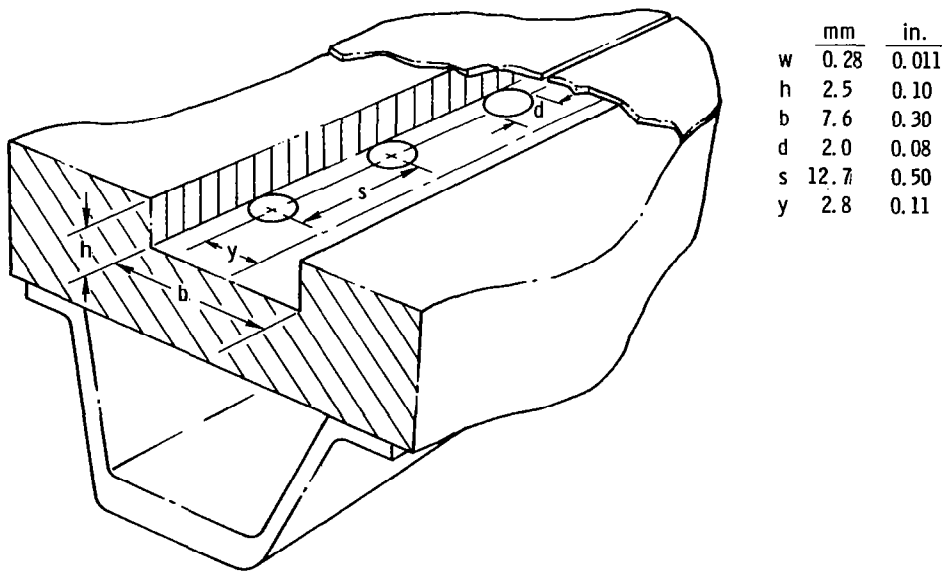


Figure 16.- Surface metering configuration.

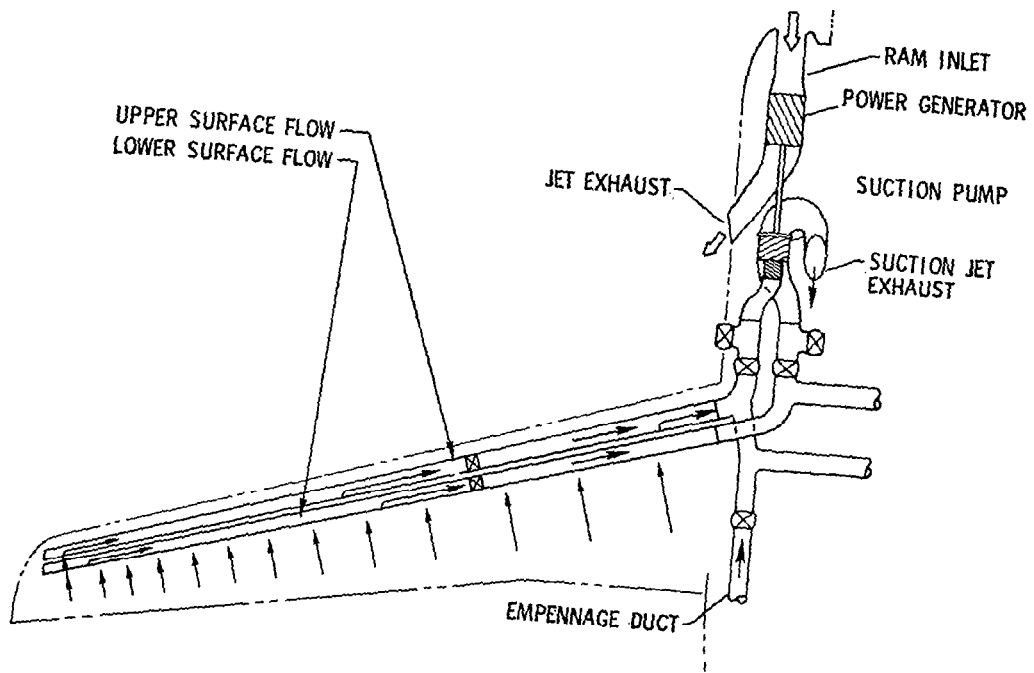


Figure 17.- Suction unit installation.

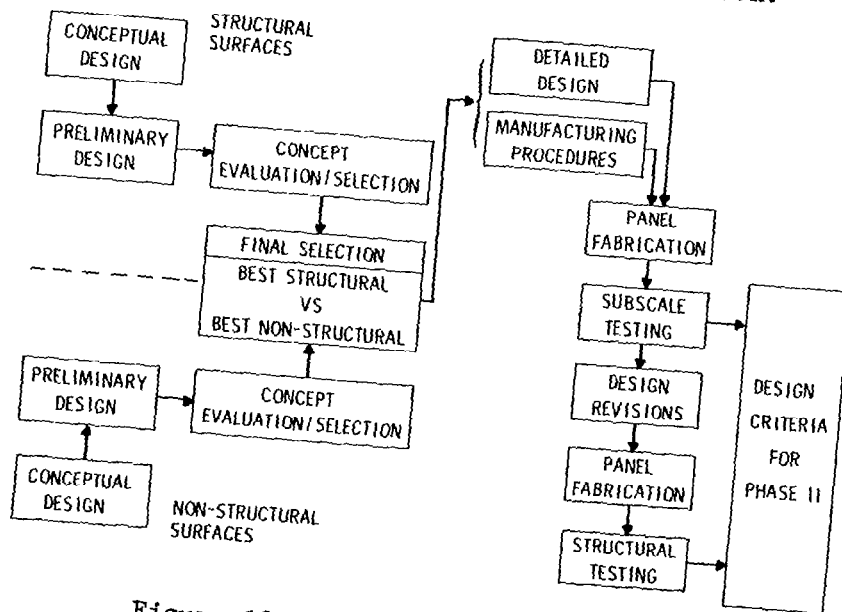


Figure 18.- LFC surface development.

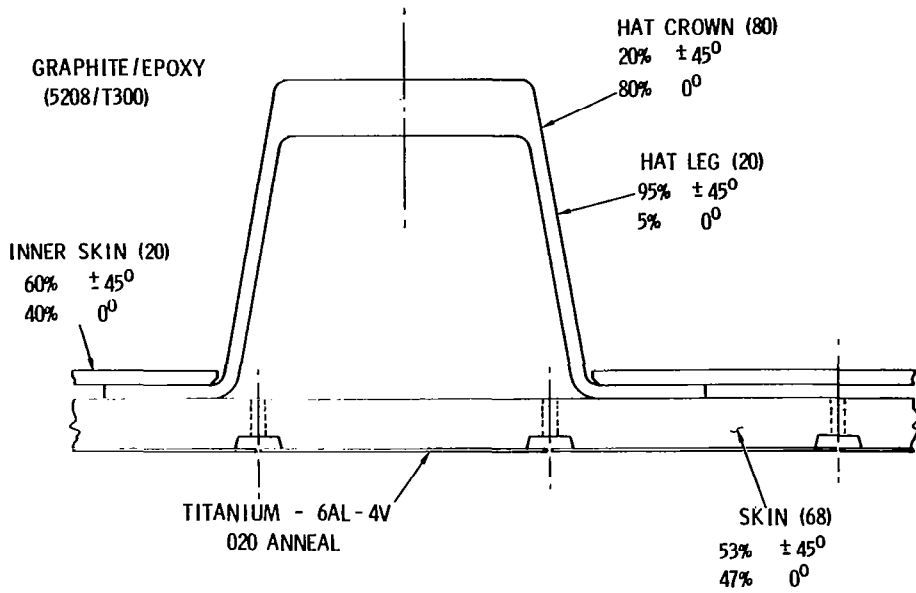


Figure 19.- Surface materials and sizing.



Figure 20.- EDM slotting of titanium.

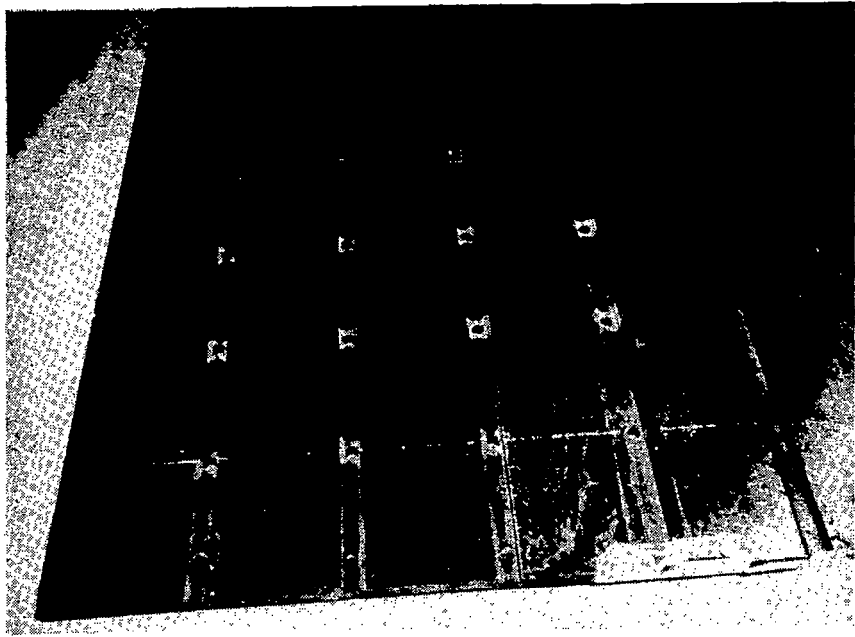


Figure 21.- Structural skin.

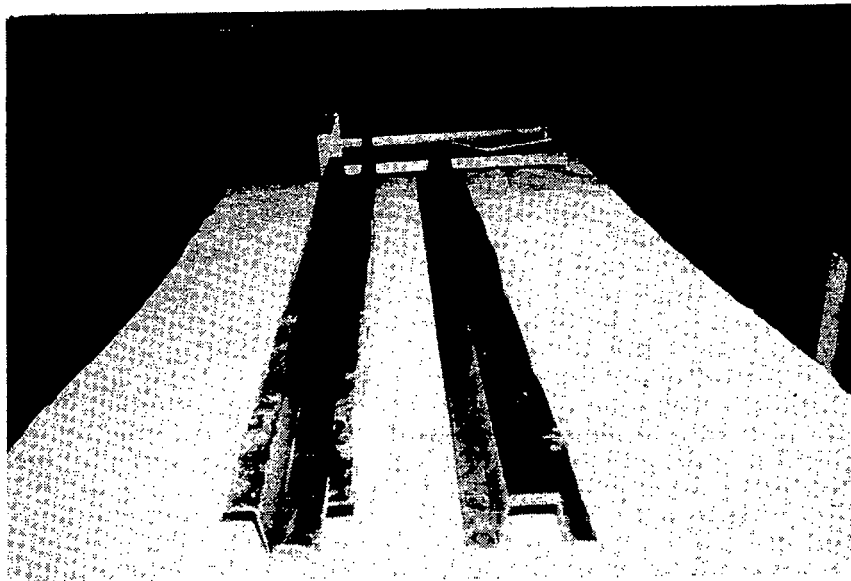


Figure 22.- Hat section stiffeners.

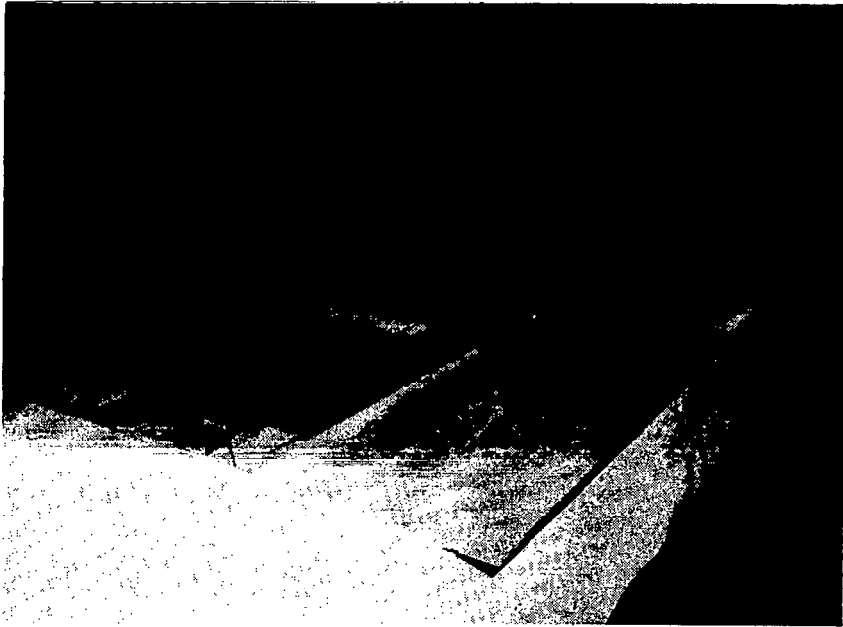


Figure 23.- Panel assembly.

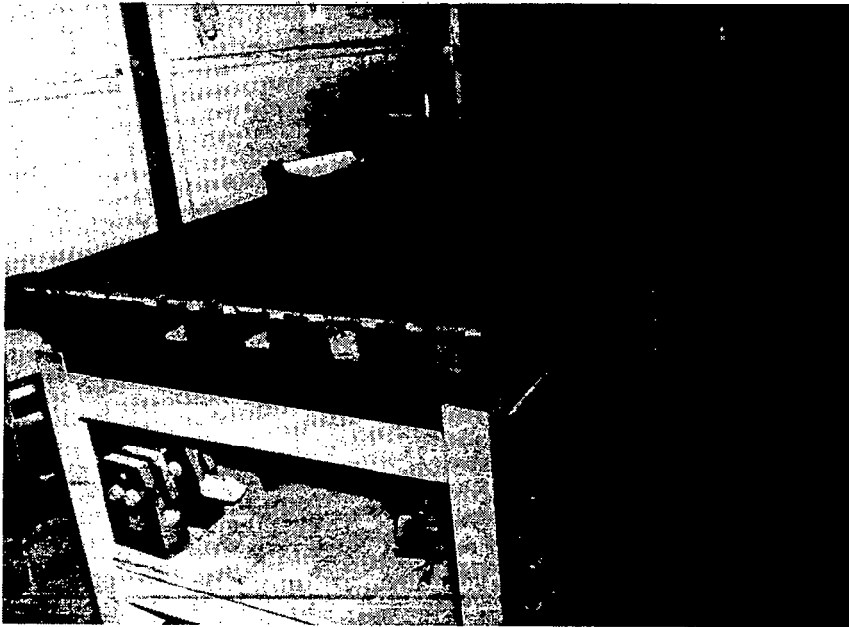


Figure 24.- Complete LFC surface panel.

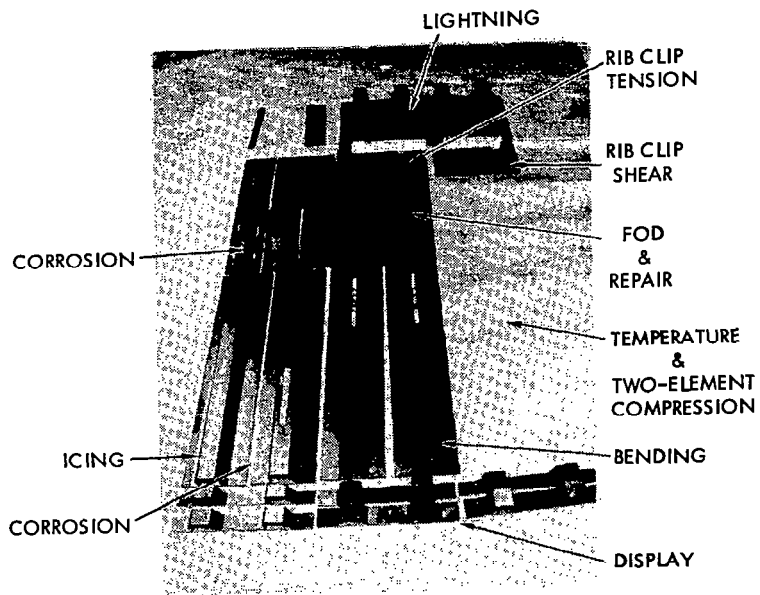


Figure 25.- Test specimens - LFC surface panel No. 1.

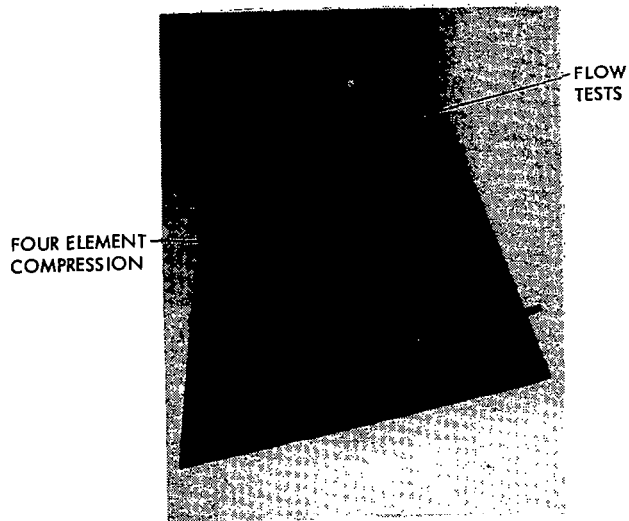


Figure 26.- Test specimens - LFC surface panel No. 2.

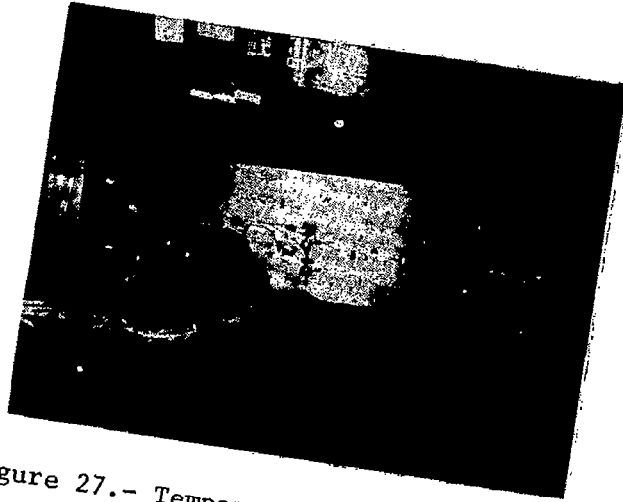


Figure 27.- Temperature test arrangement.

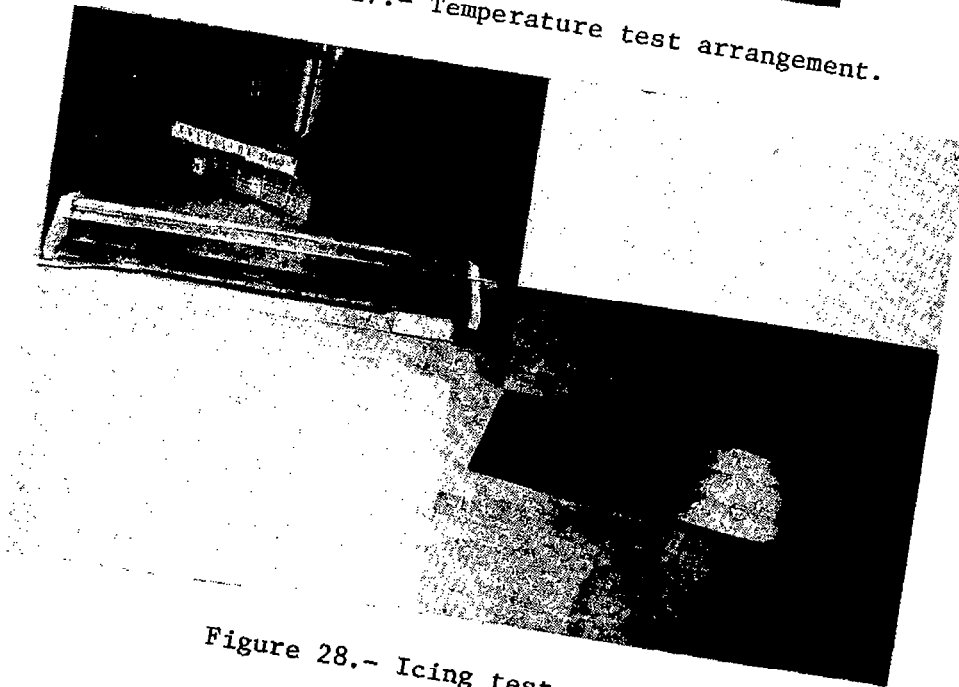


Figure 28.- Icing test specimen.

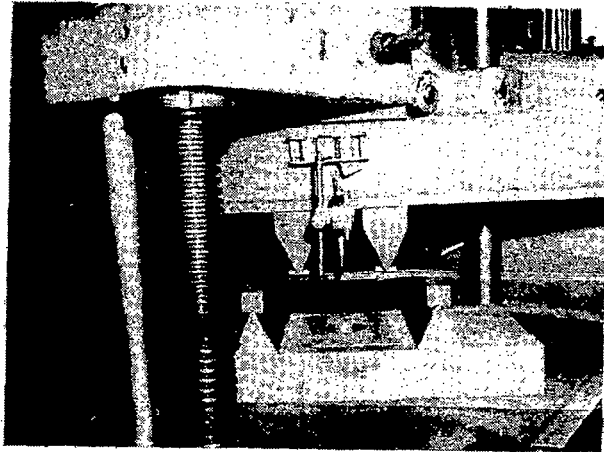


Figure 29.- Corrosion/bending test arrangement.

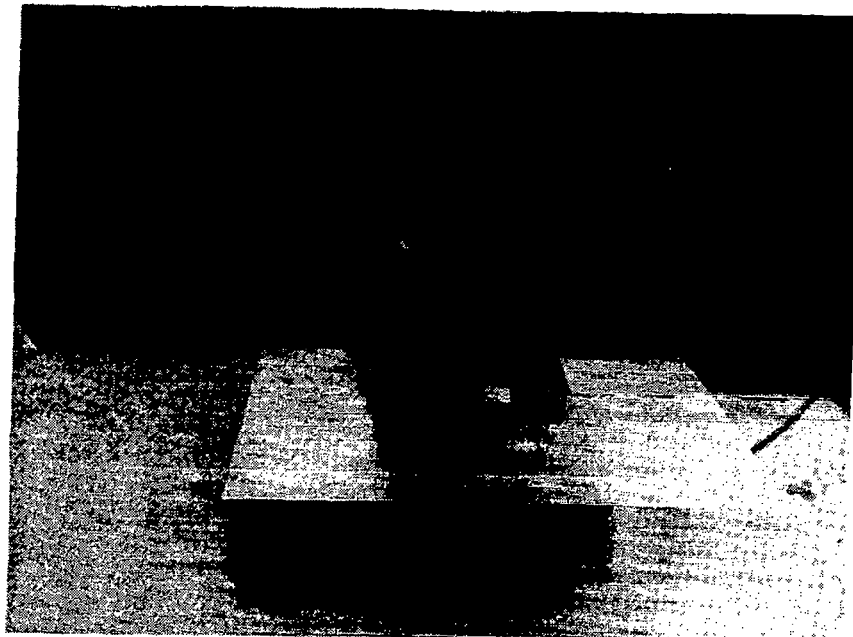


Figure 30.- Impact test arrangement.

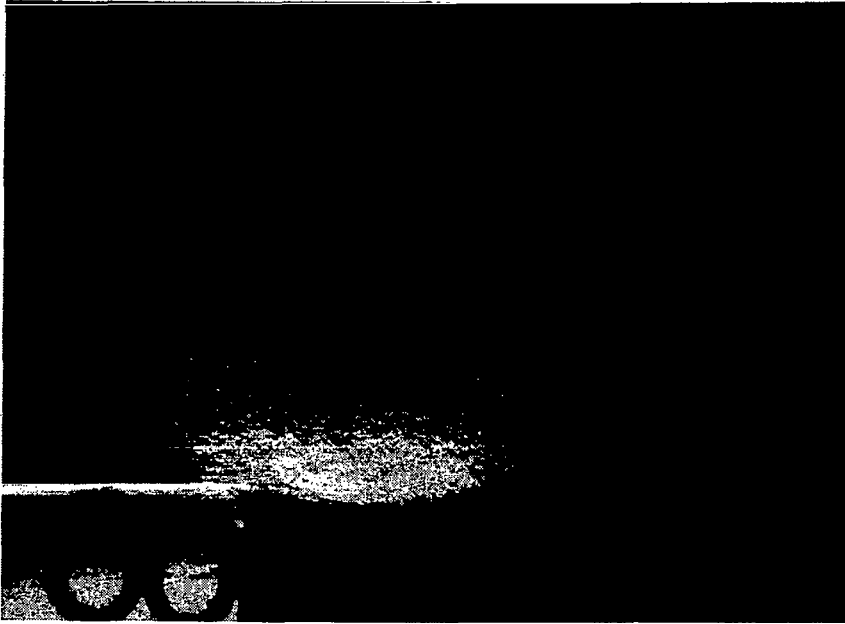


Figure 31.- Impact test specimen.

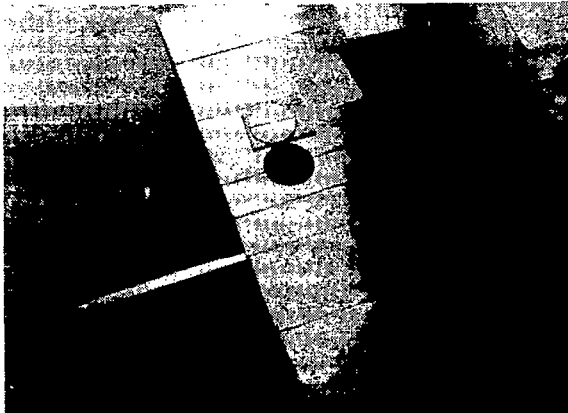


Figure 32.- Repairability test specimen.

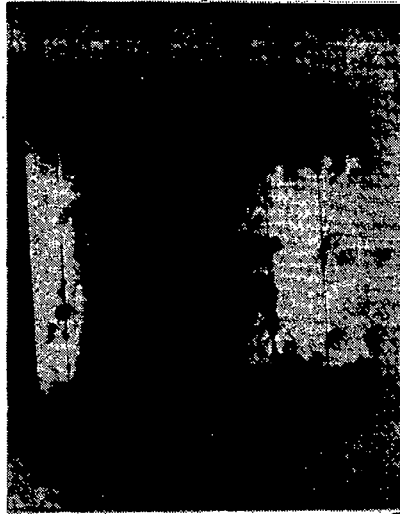


Figure 33.- Lightning test specimen.

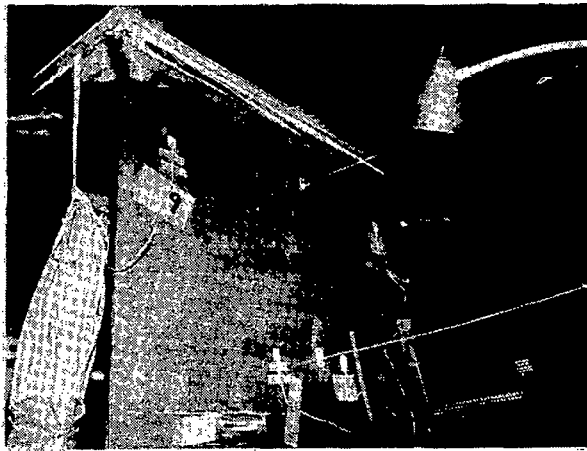


Figure 34.- Compression panel test - 1,334 MN (300,000 lb).



Figure 35.- Compression panel test - 2.224 MN (500,000 lb).

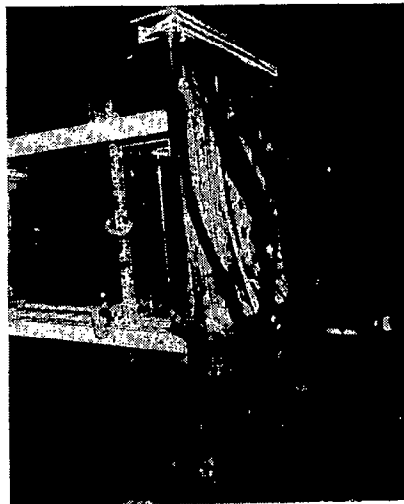


Figure 36.- Compression panel test - failure mode.